Turk J Phys
28 (2004) , 379 – 389.

Electrical Properties of Hydrogen Transport VPE Grown n-CdTe Epilayers on ZnTe/GaAs

Murat BAYHAN
Istituto Nazionale di Fisica della Materia (INFM) and Dipartimento di Ingegneria dell'Innovazione, Universitá di Lecce, Via Arnesano, I-73100 Lecce-ITALY
e-mail: mbayhan@mu.edu.tr

Received 20.11.2003

Abstract

Electrical characterisation of n-CdTe epilayers grown by hydrogen transport vapour phase epitaxy (H_2T-VPE) on insulating ZnTe/(100)GaAs substrates through the temperature dependent Hall measurements is reported. Double-crystal X-ray diffraction assessments indicate the material high crystalline quality. Samples grown at temperatures, $T_G < 650$ °C were p-type, but appeared to be n-type for the temperatures above $T_G > 650$ °C. Hall measurements performed on n-type samples of different thicknesses grown at $T_G = 764$ °C showed room temperature carrier densities in the range of 10^{11}-10^{14} cm^{-3}. The electron density and Hall mobility characteristics may be in principle well explained with a two-level affective model. The model of scattering by lattice and ionised impurity were found to be limiting dominantly the room temperature electron mobility. For a ∼22 μm thick CdTe epilayers two donor levels were mainly estimated: The first, most abundant compensates partly 10^{18} cm^{-3} density of acceptors while the second with activation energy, $E_d = 186\,meV$ determines n-type electrical properties. A compensation ratio, 0.9997 holds for this epilayer. These could be possible formed through the diffusion of Ga atoms from GaAs into CdTe.

Key Words: CdTe; Electrical properties; Hall effect; H_2T-VPE; X-ray detectors.

1. Introduction

At present efforts in the field of room temperature radiation detectors (i.e., X- and γ-ray imaging: pixellised structures) are directed towards improving both quantum efficiency and high-energy resolution [1,2] principally for use in medical imaging and high-energy X-ray astronomy [3,4]. Although inorganic scintillators coupled to photo diodes or photomultipliers often offer high stopping power, they give rather poor energy resolution. In contrast semiconductor devices such as silicon (Si) and germanium (Ge) provide excellent energy resolution. However Si offers a low stopping power for high energy photons, limiting its use to low energy photons, and Ge with a relatively small band gap requires operation at cryogenic temperatures. Consequently, cadmium telluride (CdTe) and cadmium zinc telluride (CdZnTe), with both high atomic number and high density, offer excellent spectral and spatial resolution for compact hard X-and γ-ray detection systems operating without cryogenics [5,6].

CdTe shows high quantum efficiency suitable for detection of photons in the typical range of 10 to 500 keV due mainly to relatively high atomic numbers ($Z_{Cd} = 48$, $Z_{Te} = 52$) which give a dominant photoelectric

absorption probability up to 300 keV compared to Compton scattering, and a high density resulting in good stopping power. Furthermore, its wide band gap leads to a very high resistivity (up to $10^{11}\Omega$ cm) and allows detection operation at room temperature. By comparison with silicon or germanium data (see Table 1), it is clear that CdTe has a several advantages. Finally, the intrinsic spectral resolution, simply taking into account the statistical fluctuations of the charge pulse (i.e., electron-hole pair generation) compares well with that of germanium.

Table 1. Comparison of intrinsic physical properties of some semiconducting based radiation materials, E_g is the band gap energy, ΔE_{int} is the intrinsic resolution due to statistical fluctuations of pair generation at 100 keV and E_{pair} is the ionisation potential per pair.

Material	Atomic No: Z	Density (g/cm^3)	E_g (eV)	ΔE_{int} (eV)	E_{pair} (eV)
Si	14	2.33	1.12	450	3.6
Ge	32	5.33	0.67	400	2.9
CdTe	48, 52	5.85	1.47	700	4.43
CdZnTe	48, 30, 52	5.81	1.6	620	4.6

The performance of CdTe based detectors are presently limited by low charge collection efficiency, due mainly to the poor hole mobility and the relatively small mobility lifetime product. Although high resistivity thin layers of single crystalline CdTe can be achieved by various growth techniques, the mechanisms of doping and compensation are still not well understood. Furthermore, the diameter of the CdTe crystal achieved by melt-growth methods is confined to about 1-1.5″ due to structural problems. Vapour phase crystallisation of CdTe has several advantages over melt-growth such as lower deposition temperatures, high accuracy in controlling the stoichiometry and the ease by which the compensating dopants can be introduced into the vapour. Consequently, most of the efforts have focused on the vapour phase growth of bulk CdTe, whilst vapour phase epitaxy (VPE) for the growth of detector-grade CdTe has not yet been significantly explored.

In this article, an investigation on the electrical transport mechanisms of the n-CdTe epilayers grown by H_2-VPE technique by means of temperature dependent Hall measurements is presented. Numerical analysis of the carrier density data can yield information about the levels of doping concentration, activation energy and the compensation mechanism. A comparison between the theoretical and measured values of mobility has been made to assess the nature of the scattering processes governing the mobility.

2. Experimental

The CdTe epilayers were deposited onto ZnTe/GaAs hybrid substrates by H_2-VPE technique [7]. Undoped ZnTe epilayers of $\sim 0.4\mu$m thickness required for inducing (100) nucleation of the subsequent CdTe layer were nominally grown on semi-insulating LEC-grown (110) GaAs substrates at about 350 °C using metal organic vapour phase epitaxy (MOVPE) technique. Electronic grade dimethyl-zinc and di-isopropyl-telluride were used as precursors. The ZnTe growth and the preparation of GaAs substrates are reported in detail elsewhere [8]. 5N pure CdTe powder (from Cerac, Inc) used as source material was reduced at high temperatures under 1 atm hydrogen flow prior to the growth to eliminate the native oxides from the CdTe surface. The ZnTe/GaAs samples were subsequently loaded into the H_2-VPE chamber for the CdTe growth. The source temperature was kept at 827 °C (T_S) whilst the growth temperature (T_G) was varied between 480-770 °C during all H_2T-VPE growth cycles. H_2 flow rates were around 1.0 sl/min.

Double crystal x-ray diffraction patterns (model Philips MR diffractometer employing a four-crystal channel-cut Ge (200) crystal type monochromator and a Cu-target) were obtained to evaluate the crystalline quality of CdTe epilayers. The electrical properties of the n-CdTe epilayers were evaluated by variable-temperature Hall measurements in the van der Pauw configuration. Ohmic contacts were obtained using

Au/Cr of about 300Å in thickness fabricated onto n-CdTe epilayers which were rinsed previously by diluted hydrocholoric acid to remove the native oxides.

3. Results and Discussions

3.1. Electron concentration

The analysis of the Hall data show that the CdTe epilayers grown at a source temperature of $T_G < 650$ °C were p-type and had low resistivity ($\leq 10\Omega$ cm), and their mobility and hole density was about 35-60 cm^2/Vs and (1-3) x 10^{16} cm^{-3} respectively. However, samples grown at $T_G > 650$ °C were invariably n-type with resistivities in the range of 10^2-10^6 Ω cm. Table 2 tabulates room temperature Hall data obtained from the CdTe samples (a, b, c) using the same growth temperatures, but different duration. To better understand the physical basis of the electrical features of the epilayers, temperature dependent Hall measurements were carried out on medium resistivity n-type samples (sample b). The quadratic equation (two-level effective model) for the free electron density, n, excited from a set of N_d donors of activation energy, E_d, partly compensated by the presence of N_a acceptors, is given as [9];

$$\frac{n\,(n+N_a)}{(N_d\,-\,N_a\,-n)\,N_c^o} \;=\; \beta\,(m_n^*/m_o)^{3/2}\;\exp\left(-E_d\,/kT\right) \tag{1}$$

where N_d and N_a are the concentration of donors and compensating acceptor, β is the spin degeneracy weighting factor for a donor type of flaw, m_n^* is the electron effective mass, reported in the literature for CdTe as 0.11 m_o [10], m_o is the free electron mass, $N_c^o = 2\,(2\,\pi m_o kT/h^2)^{3/2}$ is the density of states located at the conduction band edge and k and h are the Boltzmann and Planck constants respectively. This expression is valid for a single level near a parabolic conduction band and nondegenerate carrier concentrations providing that the effect of nonparabolicity of the conduction band is negligible [11].

Table 2. Room temperature resistivity (ρ), Hall coefficient (R_H), Hall mobility (μ_n) and carrier density (n) for n-type CdTe epilayers grown at $T_G = 764$ °C and $T_S = 827$ °C. d refers to the layer thickness.

Sample	d (μm)	ρ (Ωcm)	R_H ($cm^{-3}C^{-1}$)	μ_n (cm^2/Vs)	n (cm^{-3})
a	8.76	1.23 x 10^2	9.96 x 10^3	81	6.27 x 10^{14}
b	22.1	4.50 x 10^2	8.10 x 10^4	180	7.71 x 10^{13}
c	29.3	5.44 x 10^4	1.25 x 10^7	230	4.99 x 10^{11}

Figure 1 shows the log $[n\,(\,n\,+\,N_a\,)\,/\,(N_d\,-\,N_a\,-\,n)\,N_c^o]$ as a function of reciprocal temperature characteristics obtained utilizing both N_a and N_d as a free fitting parameters and n experimentally estimated for a typical medium resistivity n-type CdTe epilayer. The left-hand side of equation (1) resulted in a straight line only the correct values of N_a and N_d. The slope of the resulting straight line and the intercept at $1/T = 0$ gives the activation energy, E_d and $\beta(m_n^*/m_o)^{3/2}$ respectively. This was found to be sensitive to $N_d\,-\,N_a$ in obtaining a straight line although the data, whereas, E_d did not change noticeably for a wide choice of $N_d\,-\,N_a$. Assuming $\beta = 1/2$ for the single donor level degeneracy, the effective mass ratio may be determined as 0.16±0.01, not far from the value given for CdTe. The slope from the linear region of the characteristics and the intercept were found to be 186 meV and 0.032 for values of $N_a = 1.95x10^{15}$ cm^{-3} and $N_d = 2.32x10^{15}$ cm^{-3} respectively.

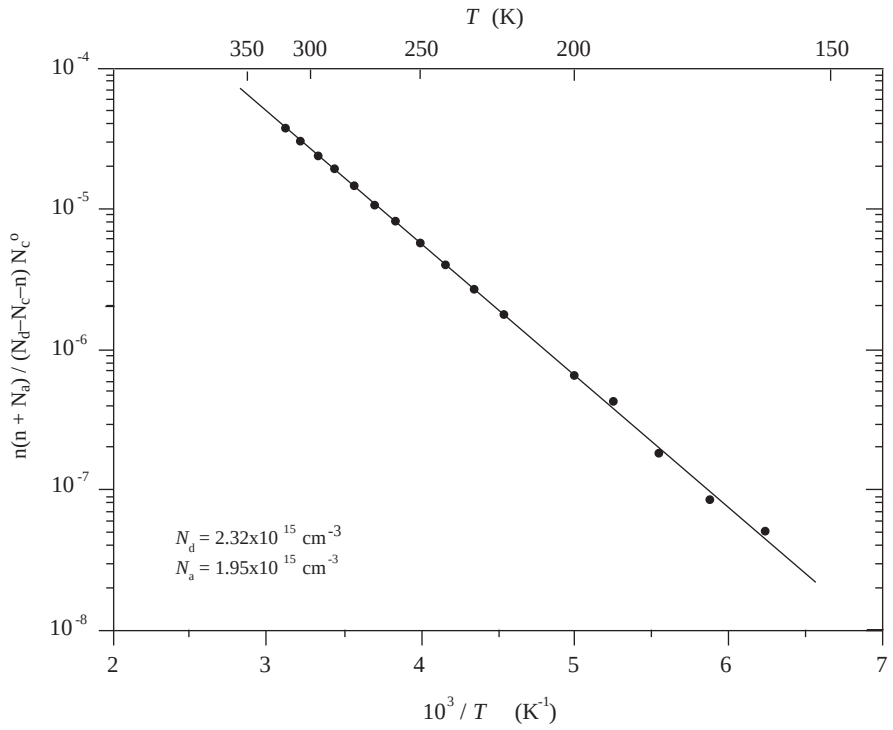

Figure 1. A plot of log $[\,n\,(\,n\,+\,N_a\,)\,/\,(N_d\,-\,N_a\,-\,n)\,N_c^o\,]$ vs. T^{-1} for a 22.1μm thick n-CdTe epilayer. The parameters, N_a and N_d employed in above are $1.95x10^{15}$cm^{-3} and $2.32x10^{15}$ cm^{-3} respectively.

Figure 2 shows the values of the free electron density obtained experimentally as function of $1/T$ (solid points). It can be seen that data fits well to the values of electron density obtained by solving the equation (1) for which the former set of parameters were employed (solid curve). A progressive decrease in the experimental values of the carrier concentration at higher temperatures compared to the that of calculated ones, could be attributed to the formation of a depleted region in the epilayer [12,13].

3.2. Carrier mobility

The dependence of the mobility on carrier concentration at relatively low temperatures allows a detailed analysis of the scattering mechanisms operating in the epilayers and to evaluate the quality of the layers further. Therefore the expected mobility values were calculated by taking into account the lattice scattering (i.e., deformation potential by acoustic phonons, polar optical phonons, piezoelectric) and impurity scattering (ionised and neutral).

Figure 3a and 3b show theoretically calculated values of electron mobility as a function of temperature due to lattice scattering (polar optical, acoustical and piezoelectric) and impurity scattering (ionised and neutral) for single crystalline n-CdTe using the Matthiessen's rule [14]. Relevant expressions for the scattering mechanisms considered in this study are given in detail in the appendix. It can be seen from the former plots that electron mobility due to piezoelectric and acoustical scattering decreased progressively with increasing temperature whilst it increased linearly with increasing temperature in the case of ionised impurity scattering. However the variation of mobility with temperature on account of neutral impurities displayed almost a steady behaviour of about 4 x 10^5 cm^2/Vs up to 200 K and thereafter increased sharply and peaked at a temperature of $\sim$ 400 K.

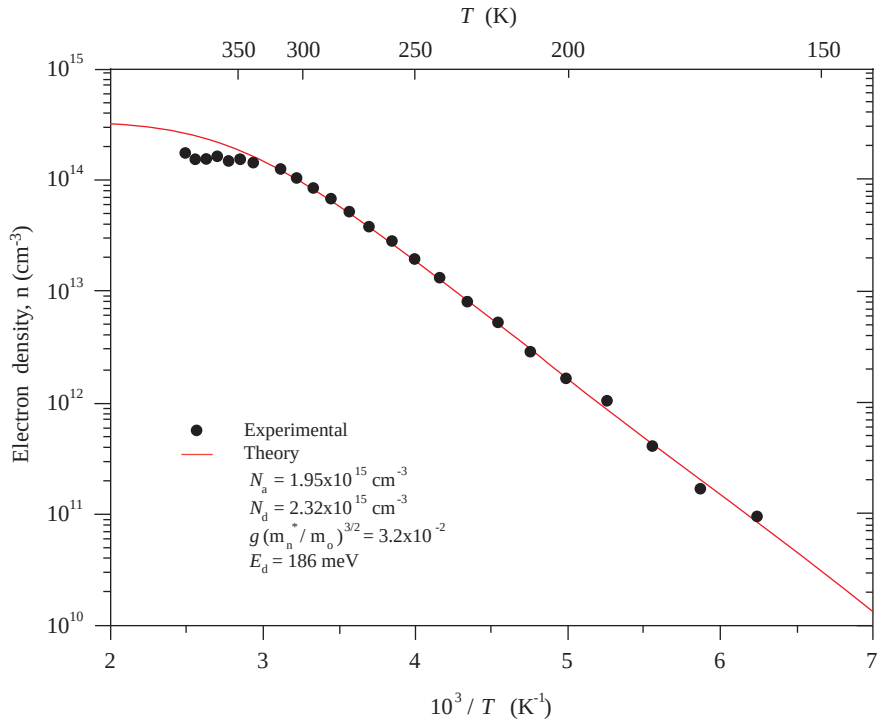

Figure 2. The logarithm of the electron density as a function of reciprocal temperature for the same layer (solid dots). The solid curve represents the electron density governed by equation (1) for a compensated extrinsic layer using appropriate values of N_a=1.95 x 10^{15}cm^{-3}, N_d=2.32 x 10^{15}cm^{-3}, β $(m_n^*/m_o)^{3/2}$=3.2 x 10^{-2} and E_d = 186 meV.

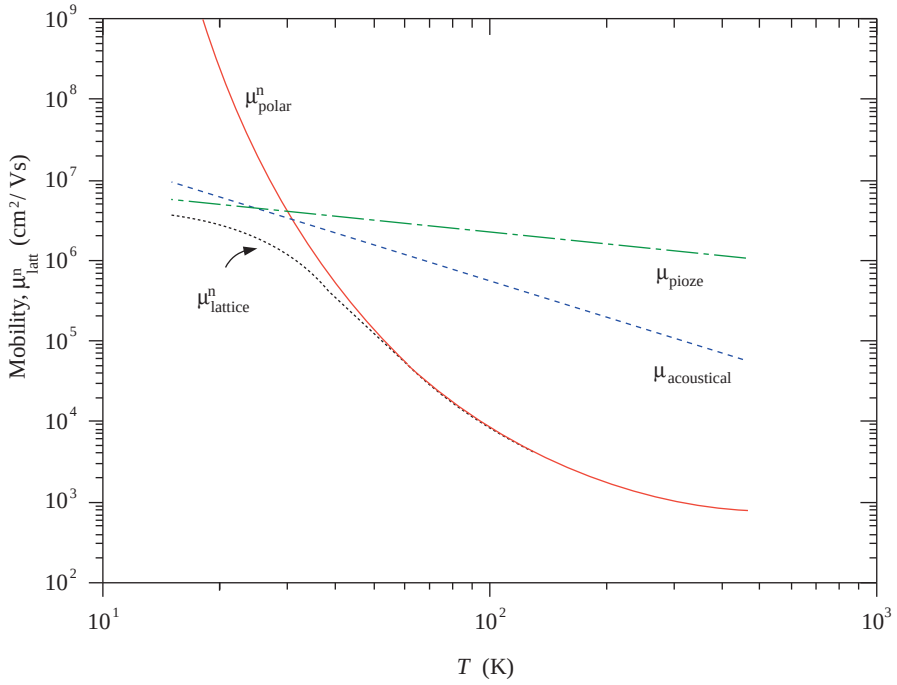

Figure 3a. Calculated electron mobility as a function of temperature due to the lattice scattering (deformation potential, polar optical phonons and piezoelectric) for crystalline n-CdTe.

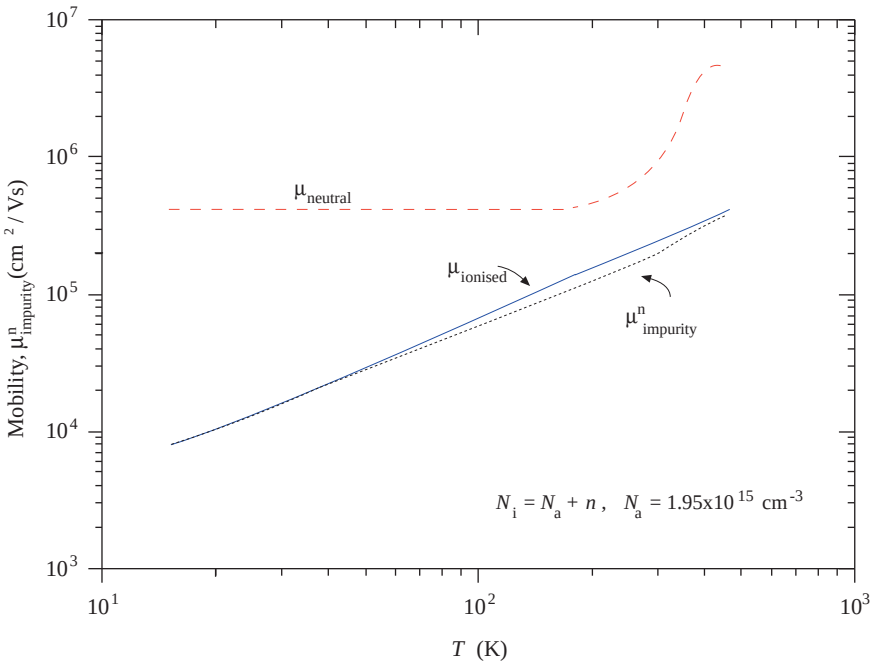

Figure 3b. Calculated electron mobility as a function of temperature due to the impurity scattering (ionised and neutral) for crystalline n-CdTe.

A log μ_n versus log T plot of mobility data displays a slope of 1.46 ± 0.19 in the range between 230 and 320 K indicating that electron mobility is dominated by ionised impurity scattering. Figure 4 displays the total lattice and ionised mobility values calculated as a function of temperature at which different values of acceptor concentration, N_a (in the range of 10^{14}-10^{20} cm^{-3}) was employed via the relation, $N_i = 2N_a + n$, where n is given by equation (1) (dashed lines) together with the measured ones (solid points). The total mobility values calculated nicely match to those obtained experimentally only if N_a is hold at 1.2 x 10^{18} cm^{-3} in the temperature range of 230–320 K.

The disagreement apparent between the two-level effective model and the electron mobility analysis could be interpreted that in addition to the above deep donor state (d) with a concentration, N_d and activation energy, E_d, a particular donor level (d1) with a concentration of N_{d1} presumably exists in the layer which partly compensates the acceptors states (i.e, $\sum_{N_a}$) leaving a residual density of $N_a = \sum_{N_a} - N_{d1} = 1.95x10^{15}$ cm^{-3} (see Figure 5). Thus the total ionised impurity concentration, N_i could be written as;

$$N_i = 2N_{d1} + 2\left(\sum_{N_a} - N_{d1}\right) + n = 2\sum_{N_a} + n \tag{2}$$

and the sample compensation ratio, K in this case can accordingly be calculated as;

$$K = \frac{\sum_{N_a}}{N_d + N_{d1}} \cong 0.9997 \tag{3}$$

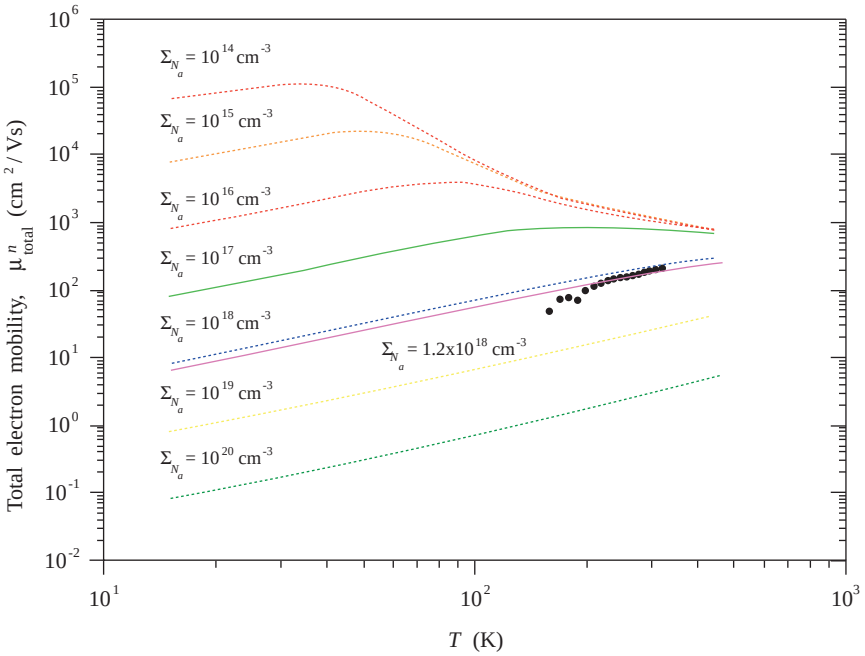

Figure 4. The total electron mobility calculated at various values of entire acceptor concentration,Σ_{N_a} (i.e., $N_i = 2\Sigma_{N_a} + n$, see the text) vs. temperature characteristics of n-CdTe epilayers (dashed lines). The circle points refer to the measured Hall mobility data.

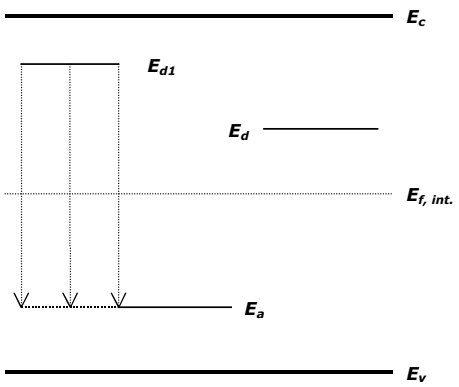

Figure 5. Schematic diagram of compensated extrinsic circumstances determined for n-CdTe epilayer (sample b in Table 2) grown by H_2-VPE method on insulating ZnTe/(100)GaAs substrates.

The above analysis indicates that scattering by lattice and ionised impurities accounted satisfactorily for the room temperature electron mobility alone, in agreement with the high crystallinity of the epilayers. The increase in the electron mobility can be thoroughly attributed to a reduction of the ionised impurity concentration at the thicker samples. Thicker epilayers appear to be less n-doped, as expected if Ga diffusion tail occurs in CdTe. In this respect, the occurrence of a dislocated CdTe region near to the CdTe/hybrid substrate interface might have somewhat enhanced the diffusion of Ga towards to the CdTe.

Ga atoms are known to introduce a shallow single donor level (Ga_{Cd}) of about 8.0 meV below the conduction band edge [15]. The d_1 donor level therefore can be well assigned to the former level, whilst the 186 meV deep d level could however, be attributed to a yet unidentified Ga-related complex. In this respect, supplementary investigations on the effect of the dislocations regarding the particular nature of the Ga doping of CdTe epilayers grown H_2T-VPE method are clearly required.

4. Conclusions

Electrical characterisation of n-CdTe epilayers grown by hydrogen transport vapour phase epitaxy (H_2T-VPE) on insulating ZnTe/(100)GaAs substrates through the temperature dependent Hall measurements is reported. Double-crystal X-ray diffraction measurements showed the sample high crystalline quality. Although the samples grown at temperatures, $T_G < 650$ °C displayed p-type features it turned n-type for the above. The Hall coefficient and mobility data of n-CdTe epilayers grown by H_2T-VPE were found to be best conform to analysis assuming two-level affective model. The Hall coefficient and the mobility data from n-CdTe epilayers grown at $T_G = 764$ °C showed electron densities in the range of 10^{11}-10^{14} cm^{-3}. For one of these samples, two distinct levels of donor mainly occurred: the most abundant one partly compensates a 10^{18} cm^{-3}density of acceptors; the second with activation energy, $E_d = 186\ meV$ determines the electrical characteristics of the layer with a residual concentration of about 10^{15} cm^{-3}. Scattering by lattice and ionised impurity accounted satisfactorily for the room temperature mobility data.

Acknowledgements

The author, M. Bayhan would like to acknowledge N. Lovergine and A. Cola for their fruitful discussions. Thanks are also due to A Pinna and C. Todisco for the technical assistance during the growth.

References

[1] P.J. Sellin, *Nucl. Instr. and Meth., A* **513**, (2003), 332.

[2] D.S. McGregor and H. Herman, *Nucl. Instr. and Meth., A* **395**, (1997), 101.

[3] T. O. Tümer, S. Yin, V. Cajipe, H. Flores, J. Mainprize, G. Mawdseley, J. Rowlands, M. Y. Yaffe, E.E. Gordon, W. J. Hamilton, D. Rhiger, S.O. Kasap, P. Sellin and K. S. Shah, *Nucl. Instr. and Meth., A* **497**, (2003), 21.

[4] S. Baba, K. Ohmori, Y. Mito, T. Tanoue, S. Yano, K. Tokumori, F. Toyofuku and S. Kanda, *Nucl. Instr. and Meth., A* **458**, (2001), 262.

[5] M. Funaki, T. Ozaki, K.Satoh, R. Ohno, *Nucl. Instr. and Meth., A* **436**, (1999), 120.

[6] O. Limousin, *Nucl. Instr. and Meth., A* **504**, (2003), 24.

[7] N. Lovergine, A. Cola, P. Prete, L.Tapfer, M. Bayhan, A.M. Mancini, *Nucl. Instr. and Meth., A* **458**, (2001), 1.

[8] G. Leo, M. Longo, N. Lovergine, A.M. Mancini, L. Vasanelli, F. Romanato, A.V. Drigo, T. Peluso, L. Tapfer, *J. Vac. Sci. Technol., B* **14 (3)**, (1996), 1739.

[9] J.S. Blakemore, *Solid State Physics*, 2nd edition (International Thomson Publishing Philadelphia, 1974) p. 320.

[10] D.T.F. Marple, *Phys. Rev.*, **129**, (1963), 2466.

[11] B. Segall, M.R. Lorenz and R.E.Halsted, *Phys. Rev.*, **129**, (1963), 2471.

[12] Y.K. Yoe, R.L. Hengehold and D.W. Elsaesser, *J. Appl. Phys.*, **61 (11)**, (1987), 5070.

[13] D.C. Look, *J. Appl. Phys.*, **66 (6)**, (1989), 2420.

[14] N. W. Ashcroft and N.D. Mermin, *Solid State Physics*, International Edition (Sounders College Publishing, China,1988) p. 323.

[15] T. Ferid and M. Saji, *J. Crystal Growth*, **172**, (1997), 83.

[16] D.J. Howart and E.H. Sondheimer, Proc. Roy. Soc. **A219**, 53 (1953).

[17] K. Seeger, *Semiconductor Physics*: *An Introduction,* 6th edition (Springer-Verlag, Berlin, 1997) p. 208.

[18] A.R. Hutson, *J. Appl. Phys. Suppl.*, **32**, (1961), 2287.

[19] H.J.G. Meyer and D.Polder, *Physica*, **19**, (1953), 255.

[20] J. Bardeen and W. Shockley, *Phys. Rev.*, **80**, (1950), 72.

[21] H. Brooks: *Advances in Electronics and Electron Physics,* ed. L. Marton, vol. 7 (Academic Press, New York, 1955) p. 85.

[22] E. Conwell, V.F. Weisskopf, *Phys. Rev.*, **77**, (1950), 388.

[23] C. Erginsoy, *Phys. Rev.*, **79**, (1950), 1013.

[24] C. Schwartz, *Phys. Rev.*, **124**, (1961), 1468.

Appendix

The following expressions were employed for the lattice scattering (polar optical phonon, piezoelectric and acoustical deformation potential).

i- Polar optical phonon scattering [16,17]:

$$\mu_{po} \;=\; \frac{4e}{3\,\alpha\,w_l\,m_n^*\;\pi^{1/2}}\;\;\frac{G\,(\theta_D\,/T)\;[\exp\,(\theta_D/T\,)\;-1\,]}{(\;\theta_D\,/\,T\,)^{\,1\,/\,2}} \tag{A1}$$

where w_l is the angular frequency of the longitudinal optical phonon and α is the polaron coupling constant and is defined as;

$$\alpha = \frac{\hbar e\,E_o}{2\,m_n^{*\;1/2}(\hbar w_l)^{3/2}} \tag{A1a}$$

respectively. E_o is called effective field strength and is given by;

$$E_o = \frac{e\,m_n^*\,k\,\theta_D}{4\,\pi\,\varepsilon_o\,\hbar^{\,2}}\;\;\left(\,\varepsilon_{\,r,\,\infty}^{\;-1}\;-\;\;\varepsilon_{\,r,\,s}^{\;-1}\,\right) \tag{A1b}$$

where θ_D is the Debye temperature, $\varepsilon_{r,\,\infty}$, $\varepsilon_{r,\,s}$ and ε_o are the relative infinite, static and free space dielectric constants respectively. It should be noted that the function, $G\,(\theta_D/T)$ obtained by Fortini et all was employed in equation (A1) and the values of Debye temperature, relative dielectric constants and electron effective mass were taken as $\theta_D = 252\,^oK$, $\varepsilon_{r,\,\infty} = 10.2$, $\varepsilon_{r,\,s} = 7.2$ and $0.11m_o$ respectively.

ii- Piezoelectric scattering [18,19]:

$$\mu_{pz} \;=\; \frac{16\,(2\pi\,)^{1\,/\,2}}{3}\;\;\frac{\hbar^2\,\varepsilon_o\,\varepsilon_{r,\,s}}{m_n^{*\;3/2}\;e\;K^2\;\;(k\,T)^{1\,/\,2}} \tag{A2}$$

where K^2 is electro-mechanical coupling coefficient and defined as;

$$K^2 \;=\; \frac{e_{pz}^2\,/c_l}{\varepsilon_o\,\varepsilon_{r,\,s}\;+\;\;e_{pz}^2\,/\,c_l} \tag{A2a}$$

where e_{pz}^2 is the piozeelectric constant, c_l is the longitudional elastic constant and is given for a [100] direction of wave propagation in a cubic lattice, $c_l \;=\; c_{11}$, for a [110] direction $c_l \;=\; (\,c_{11}\;+\;c_{12}\;+\;c_{44})\,/2$, and for a [111] direction $c_l = \;(\,c_{11}\;+\;2c_{12}\;+\;4c_{44})\,/3$ respectively.

iii- Acoustical deformation potential scattering [20]:

$$\mu_{ac} \;=\; \frac{2\,(2\,\pi\,)^{1\,/\,2}}{3}\;\;\frac{e\,\hbar^4\,c_l}{m_n^{*\;5/2}\,k^{3/2}\,E_{ac}^2\,T^{3/2}} \tag{A3}$$

where E_{ac} is called acoustical deformation potential and is about 4.45 eV for CdTe. For the impurity scattering (ionised and neutral) the following equations were namely used;

i- ionised impurity scattering [21,22]:

$$\mu_{ionised} \;=\; \frac{2^{\,7/2}\;(4\pi\,\varepsilon_{r,\,s}\,\varepsilon_o\,)^2\,(k\,T)^{3/2}}{\pi^{\,3/2}\,Z^2\,e^3\,m_n^{*\;1/2}\,N_i\left[\ln\,(1+\beta_{BH}^2)\;\;-\;\;\frac{\beta_{BH}^2}{(1+\beta_{BH}^2)}\right]} \tag{A4}$$

where β denoted β_{BH} in which B and H are the initials of Brooks and Herring is given by;

$$\beta_{BH}^2 \;=\; 24\;(m_n^*/\hbar^2)\,k\,T\,L_D^2 \tag{A4a}$$

where L_D is the Debye length and is given by;

$$L_D^2 = (kT/e^2)\,(\varepsilon_{r,s}\,\varepsilon_o\,/n'\,) \tag{A4b}$$

where $n' = n + (n + N_a)\,[1 - (n + N_a)\,/\,N_d]$ is the effective electron density and $N_i = 2N_a + n$ is the ionised impurity concentration.

ii- Neutral impurity scattering [23,24]:

$$\mu_{neutral} = \frac{e\,(m_n^*/\,m_o\,)}{20\;a_B\,\hbar\,\varepsilon_{r,\,s}\,N_N} \tag{A5}$$

where $N_N = N_d - N_a - n$ is the neutral impurity concentration and a_B is the Bohr radius.